

# Hybrid Message Passing-Based Detectors for Uplink Grant-Free NOMA Systems

Yi Song, Yiwen Zhu, Kun Chen-Hu, *Member, IEEE*, Xinhua Lu, Peng Sun\*, Zhongyong Wang

**Abstract**—This paper studies improving the detector performance which considers the activity state (AS) temporal correlation of the user equipments (UEs) in the time domain under the uplink grant-free non-orthogonal multiple access (GF-NOMA) system. The Bernoulli Gaussian-Markov chain (BG-MC) probability model is used for exploiting both the sparsity and slow change characteristic of the AS of the UE. The GAMP Bernoulli Gaussian-Markov chain (GAMP-BG-MC) algorithm is proposed to improve the detector performance, which can utilize the bidirectional message passing between the neighboring time slots to fully exploit the temporally-correlated AS of the UE. Furthermore, the parameters of the BG-MC model can be updated adaptively during the estimation procedure with unknown system statistics. Simulation results show that the proposed algorithm can improve the detection accuracy compared with the existing methods while keeping the same order complexity.

**Index Terms**—Uplink GF-NOMA detectors, temporally-correlated UE activity state, hybrid message passing, GAMP.

## I. INTRODUCTION

THE Massive machine-type communications (mMTC) is one of the key pillars of the next 6th-generation (6G) cellular networks for Internet of Things (IoT) applications [1]. In mMTC scenario, the central base station (BS) is serving billions of UEs, and both spectral efficiency and low-latency must be satisfied by a multiple-access scheme. The GF-NOMA is a promising candidate to support mMTC. The NOMA technique enables the system resource block to simultaneously serve multiple UEs [2], while the grant-free (GF) scheme allows UEs to transmit data to the BS directly without waiting for its permission, which can decrease the access delay and reduce the control overhead for coordination [3].

In the case of applying GF-NOMA to uplink, recovering the transmitted signal through designing efficient multi-UEs detection methods is challenging, not only due to the large number of the UEs present in the cell, but they are also randomly accessing to the network in each access slot. However, UEs are only sporadically and randomly activated in the practical mMTC systems, which brings sparsity of the transmitted slots in the time-frequency resource grid [4], and this sparsity can be changed across different slots within a single frame [5], [6]. Furthermore, once a UE is activated for performing the data transmission, it typically requires several

consecutive time slots. Then, this UE will be deactivated for a certain period till the next transmission. This activation and deactivation is denoted as AS, and it exhibits a temporal correlation [7]. Consequently, to enhance the performance of the detectors based on a GF-NOMA system, not only the joint exploitation of sparsity but also the temporal correlation information provided by AS in the system.

According to the literature of GF-NOMA, detectors based on message passing (MP) algorithms [6]–[8] have a better performance as compared to the conventional compressed sensing (CS) methods. In [6], the authors exploited the temporal correlation of the active UE and modeled by a Markov process. The authors in [7] utilized the sparse Bayesian learning (SBL) and pattern coupled sparse Bayesian learning (PCSBL) model to formulate the slow change of the UEs AS, then proposed the SBL-based multi-UEs detection algorithms outperforming CS methods. Then [8] further embedded the generalized approximate message passing (GAMP) algorithm with the SBL, PCSBL models, and proposed the GAMP sparse Bayesian learning (GAMP-SBL) and the GAMP pattern coupled sparse Bayesian learning (GAMP-PCSBL) detector algorithms, which can reduce the complexity. However, the SBL and PCSBL models mainly consider the sparse structure of the UE activity. Motivated by [6], we find that the Markov chain (MC) better captures the slow change of the AS features with successive time slots and the active UE sparsity simultaneously. Further different with [6], we use the hybrid message passing (HMP) rule [9] to update the parameters of the MC on the factor graph (FG), to improve the convergence speed.

In this paper, we focus on designing a high-performance MP algorithm and resulting in the GAMP-BG-MC detector algorithm for the uplink GF-NOMA system. The main contributions of this paper are summarized as follows.

- 1) We employ the BG-MC model [10] to fully exploit both the sparse structure of the active UE and the slow change feature in consecutive time slots of the AS. Indeed, we can improve the detector performance by updating the AS by considering the temporal correlation. Hence, both the forward messages from the previous slot and the backward messages from the next slot are considered in the MP algorithm at each iteration.
- 2) Making use of the HMP rule, we proposed the GAMP-BG-MC algorithm to detect the received signal of multiple superimposed UEs. The proposed GAMP-BG-MC algorithm not only calculates the more accurate posterior probability density function (PDF) of the transmitted signal but also adaptively learns the parameters of the prior model during the estimation procedure. Simula-

Y. Song, Y. Zhu, P. Sun and Z. Wang are with the School of Electrical and Information Engineering, Zhengzhou University, 450001, Zhengzhou, China (songyizzu@gs.zzu.edu.cn; zhuyw@gs.zzu.edu.cn; iepeng-sun@zzu.edu.cn; iezzywang@zzu.edu.cn). K. Chen-Hu is with the Department of Electronic Systems, Aalborg University, 9220, Aalborg, Denmark (kchenhu@es.aau.dk). X. Lu is with the College of Information Engineering, Nanyang Institute of Technology, 473000, Nanyang, China (ieluxinhua@sina.com).

tion results show that the GAMP-BG-MC algorithm has a better signal-to-noise ratio (SNR) performance as compared to the GAMP-SBL [7], [8] and the GAMP-PCSBL [8] algorithms respectively while keeping the complexity.

## II. SYSTEM MODEL AND FACTOR GRAPH

### A. System Model

We consider a typical GF-NOMA system [8], where  $K$  potential single-antenna UEs share the same bandwidth resource and transmit the signal to the central BS is equipped with a single antenna, as illustrated in Fig. 1. We assume that the transmission utilizes the multi-carrier code division multiple access (MC-CDMA) scheme detailed in [11], which belongs to the non-orthogonal multiple access (NOMA) techniques. The MC-CDMA is a hybrid scheme combining code division multiple access (CDMA) and orthogonal frequency-division multiplexing (OFDM), makes the MC-CDMA signal tolerant against frequency selective channels, inter-symbol interference (ISI) and inter-carrier interference (ICI) through the use of cyclic prefix and equalization [12]. The uplink transmission of the UEs is multiplexed over  $N$  frequency-divided subcarriers. In each time slot, we assume the AS of different UEs are independent of each other,  $K_a \leq K$  of which are active and transmit packets to the BS. We use the active rate  $p_a$  to indicate the percentage of active UEs. The active UE  $k$  sends the complex symbol  $b_k$  from a predefined complex signal constellation, and spreads it over the  $N$  sub-carriers. While the inactive UE is considered transmitting a zero symbol  $b_k = 0$ . The received signal  $\mathbf{y} = [y_1, \dots, y_N]^T$  at the BS for the  $j$ -th time slot can be expressed as

$$\mathbf{y} = \mathbf{H}\mathbf{b} + \mathbf{w}, \quad (1)$$

where  $\mathbf{H} = [\mathbf{h}_1, \dots, \mathbf{h}_K] \in \mathbb{C}^{N \times K}$  denotes the complex channel response matrix, representing the spread codes of  $K$  UEs over  $N$  sub-carriers.  $\mathbf{b} = [b_1, \dots, b_K]^T$  is the transmitted signal from  $K$  UEs.  $\mathbf{w} = [w_1, \dots, w_N]^T \sim \mathcal{CN}(\mathbf{0}, \lambda^{-1}\mathbf{I})$  denotes the additive white Gaussian noise (AWGN) with the variance  $\lambda^{-1}$ . The received signals  $\mathbf{Y} = [\mathbf{y}_1, \dots, \mathbf{y}_J] \in \mathbb{C}^{N \times J}$  collect  $J$  continuous time slots and represent as a multiple measurement vector (MMV) model [8]

$$\mathbf{Y} = \mathbf{H}\mathbf{B} + \mathbf{W}, \quad (2)$$

where  $\mathbf{B} = [\mathbf{b}_1, \dots, \mathbf{b}_J] \in \mathbb{C}^{K \times J}$  denotes the transmitted signal matrix, and the noise is  $\mathbf{W} = [\mathbf{w}_1, \dots, \mathbf{w}_J] \in \mathbb{C}^{N \times J}$ . In a practical mMTC scenario, the potential UEs keep their AS in some random consecutive time slots within the entire frame [4]. As shown in Fig. 1, the AS of the UE exhibits the temporal correlation in the time domain, which promotes the sparse structure of signal  $\mathbf{B}$  in (2). The task of multi-UEs detection is to estimate the sparse transmitted signal  $\mathbf{B}$  from the received signal  $\mathbf{Y}$  with the unknown UE activity value.

### B. Probabilistic Formulation

From (2), we define the hidden variable  $\mathbf{Z} \triangleq \mathbf{H}\mathbf{B} \in \mathbb{C}^{N \times J}$ , in which  $\mathbf{z}_j = \mathbf{H}\mathbf{b}_j, \forall j \in J$ . Then the detector transfer function can be written as

$$p(\mathbf{Y}|\mathbf{B}) = p(\mathbf{Y}|\mathbf{Z})p(\mathbf{Z}|\mathbf{B}) = \prod_{j=1}^J p(\mathbf{y}_j|\mathbf{z}_j)p(\mathbf{z}_j|\mathbf{b}_j). \quad (3)$$

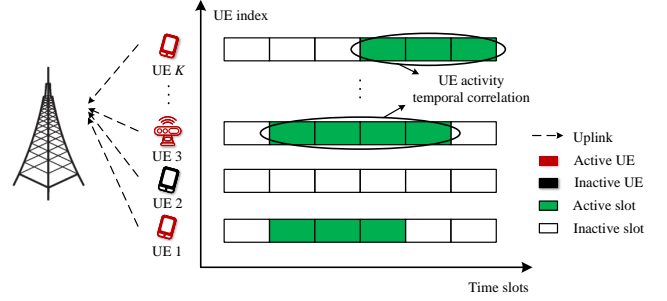


Fig. 1: The left part of the figure denotes the uplink transmission from UEs to the BS; The right part of the figure indicates the sparse and temporally correlated structures of the transmit signal  $\mathbf{B}$ .

The conditional PDF  $p(\mathbf{y}_j|\mathbf{z}_j)$  can be further factorized as

$$p(\mathbf{y}_j|\mathbf{z}_j) = \prod_{n=1}^N \underbrace{p(y_{n,j}|z_{n,j})}_{f_{Y,n,j}} = \prod_{n=1}^N \mathcal{CN}(y_{n,j}; z_{n,j}, \lambda^{-1}). \quad (4)$$

The hard constraint factors provided by  $p(\mathbf{z}_j|\mathbf{b}_j)$  can be concretely represented as

$$p(\mathbf{z}_j|\mathbf{b}_j) = \prod_{n=1}^N \underbrace{p(z_{n,j}|\mathbf{b}_j)}_{f_{Z,n,j}} = \prod_{n=1}^N \delta\left(z_{n,j} - \sum_{k=1}^K h_{n,k} b_{k,j}\right), \quad (5)$$

where the  $h_{n,k}$  denotes the element in the  $n$ -th row and  $k$ -th column of  $\mathbf{H}$ .

For the channel prior model, we utilize the BG-MC probability model [10], which can exploit both the block sparse structure and slow change of the UE AS feature simultaneously. Each element  $b_{k,j}$  has a conditionally independent distribution given by

$$\begin{aligned} p(\mathbf{B}|\mathbf{S}, \mathbf{V}) &= \prod_{k=1}^K \prod_{j=1}^J \underbrace{p(b_{k,j} | s_{k,j}, v_{k,j})}_{f_{B,k,j}} \\ &= \delta(s_{k,j})\delta(b_{k,j}) + \delta(1 - s_{k,j})\mathcal{CN}(b_{k,j}; 0, v_{k,j}^{-1}), \end{aligned} \quad (6)$$

where  $s_{k,j} \in \{0, 1\}$  denotes the MC state implicating if the UE is active ( $s_{k,j} = 1$ ) or inactive ( $s_{k,j} = 0$ ) at the  $j$  time slot;  $v_{k,j}^{-1}$  is non-negative hyperparameter controlling the sparsity of the transmitted signal  $b_{k,j}$ .

Similar to [6], [10], [13], we employ the stationary first-order MC to effectively capture the slow evolution of UE AS across time slots. The MC here given by

$$p(\mathbf{S}) = \prod_{k=1}^K p(\mathbf{s}_k) = \prod_{k=1}^K \underbrace{[p(s_{k,1})]}_{f_{S,k,1}} \prod_{j=2}^J \underbrace{p(s_{k,j}|s_{k,j-1})}_{f_{S,k,j}}, \quad (7)$$

with the initial probability given by  $p(s_{k,1}) = (p_k^{10})^{s_{k,1}}(1 - p_k^{10})^{1-s_{k,1}}$  and the transition probability is expressed as

$$p(s_{k,j}|s_{k,j-1}) = \begin{cases} (1 - p_k^{10})^{1-s_{k,j}}(p_k^{10})^{s_{k,j}}, & s_{k,j-1} = 0, \\ (p_k^{01})^{1-s_{k,j}}(1 - p_k^{01})^{s_{k,j}}, & s_{k,j-1} = 1, \end{cases} \quad (8)$$

The MC is characterized by parameters  $p_k^{01} \triangleq \Pr(s_{k,j} = 0|s_{k,j-1} = 1)$  and  $p_k^{10} \triangleq \Pr(s_{k,j} = 1|s_{k,j-1} = 0)$  for different UEs. Different from [6], [10], we consider the

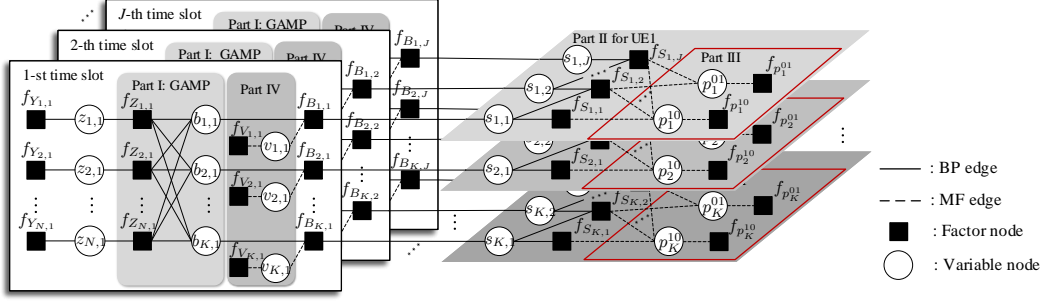


Fig. 2: Factor graph representation for the GF-NOMA detectors.

parameters  $p_k^{01}, p_k^{10}$  as variables, and the prior given by the Beta distributions as

$$\underbrace{p(p_k^{01})}_{f_{p_k^{01}}} = \text{Be}(p_k^{01}; c_k, d_k), \underbrace{p(p_k^{10})}_{f_{p_k^{10}}} = \text{Be}(p_k^{10}; e_k, f_k), \quad (9)$$

where  $c_k, d_k$  and  $e_k, f_k$  can control the initial values of  $p_k^{01}$  and  $p_k^{10}$ , respectively. Meanwhile, the precision terms  $v_{k,j}$  can be modeled as the Gamma distribution [14], i.e.,

$$p(\mathbf{V}) = \prod_{k=1}^K \prod_{j=1}^J \underbrace{p(v_{k,j})}_{f_{v_{k,j}}} = \prod_{k=1}^K \prod_{j=1}^J \text{Ga}(v_{k,j}; \epsilon_{k,j}, \eta_{k,j}), \quad (10)$$

where the initial values of  $v_{k,j}$  controlled by  $\epsilon_{k,j}, \eta_{k,j}$ .

### C. Factor Graph Representation

Based on (2), (4)-(10), the joint PDF of all unknown variables given by the observation  $\mathbf{Y}$  can be factorized as

$$\begin{aligned} & p(\mathbf{B}, \mathbf{Z}, \mathbf{S}, \mathbf{V}, \mathbf{p}^{10}, \mathbf{p}^{01} | \mathbf{Y}) \\ &= p(\mathbf{Y} | \mathbf{Z}) p(\mathbf{Z} | \mathbf{B}) p(\mathbf{B} | \mathbf{S}, \mathbf{V}, \mathbf{p}^{10}, \mathbf{p}^{01}) \\ &\propto \prod_{j=1}^J \left\{ \prod_{n=1}^N f_{Y,n,j}(y_{n,j}, z_{n,j}) f_{Z,n,j}(z_{n,j}, \mathbf{b}_j) \prod_{k=1}^K \right. \\ &\quad \left. f_{B_{k,j}}(b_{k,j}, s_{k,j}, v_{k,j}) f_{v_{k,j}}(v_{k,j}) \right\} \prod_{k=1}^K \left\{ f_{p_k^{01}}(p_k^{01}) f_{p_k^{10}}(p_k^{10}) \right. \\ &\quad \left. f_{S_{k,1}}(s_{k,1}, p_k^{10}) \prod_{j=2}^J f_{S_{k,j}}(s_{k,j}, s_{k,j-1}, p_k^{10}, p_k^{01}) \right\}. \quad (11) \end{aligned}$$

The factor graph of (11) is illustrated in Fig. 2.

## III. ADAPTIVE DETECTOR BASED ON THE HMP RULE

In this section, we utilize the efficient GAMP algorithm to obtain the likelihood function for the signal  $b_{k,j}, \forall k, j$ . We propose the novel GAMP-BG-MC algorithm, which can adaptively update the parameters and get the accurate marginal posterior PDF.

### A. Computation of the HMP for GAMP-BG-MC algorithm

The probability model in (6) implicit the mix of linear and non-linear functional relationships, i.e., the product and summation operations among the variables as well as the updating of the Gaussian variance. While the single or combined MP

rules are unavailable to calculate all the messages directly. Fortunately, the HMP rule proposed in [9], can tackle the message computation problems with the mix of linear and nonlinear models. The idea of the HMP rule [9] is that: the FG groups all factor nodes into one set  $\mathcal{A}_{\text{Hybrid}}$ , while clusters all edges  $\mathcal{E}$  into two sets:  $\mathcal{E}_{\text{BP}}$  and  $\mathcal{E}_{\text{MF}}$ , depicted as solid and dashed lines in Fig. 2, respectively. For  $\mathcal{E}_{\text{BP}}$  edges, we use the equations [9, eqs. (5), (6)] to calculate the messages. Consequently, [9, eqs. (7), (8) and (9)] are used to calculate the messages on the  $\mathcal{E}_{\text{MF}}$ . For the convenience of MP algorithm design, we divide the factor graph into four parts as shown in Fig. 2. Then, we will derive the message separately.

*Part 1 - GAMP part messages:* The GAMP algorithm is used to obtain the likelihood messages  $n_{b_{k,j} \rightarrow f_{B_{k,j}}}^{\text{BP}}(b_{k,j}) = \mathcal{CN}(b_{k,j}; \hat{q}_{k,j}, v_{q_{k,j}})$  of the variable  $b_{k,j}$ . The detailed scheme of the GAMP algorithm can be found in [15, Algorithm 1]. We first initialize the beliefs  $b(v_{k,j}) = \text{Ga}(v_{k,j}; \hat{\epsilon}_{k,j}, \hat{\eta}_{k,j})$ , whose parameters are updated in (27). Then,  $m_{f_{B_{k,j}} \rightarrow s_{k,j}}^{\text{BP}}(s_{k,j})$  can be calculated by the HMP rule [9, eq. (5)], resulting in

$$m_{f_{B_{k,j}} \rightarrow s_{k,j}}^{\text{BP}}(s_{k,j}) = \bar{\pi}_{k,j} \delta(1 - s_{k,j}) + (1 - \bar{\pi}_{k,j}) \delta(s_{k,j}), \quad (12)$$

where

$$\begin{cases} \bar{\pi}_{k,j} = \frac{\text{temp}_{k,j}}{\text{temp}_{k,j} + 1}, \\ \text{temp}_{k,j} \triangleq \frac{e^{\psi(\hat{\epsilon}_{k,j})} \mathcal{CN}(\hat{q}_{k,j}; 0, v_{q_{k,j}} + \hat{\eta}_{k,j} / \hat{\epsilon}_{k,j})}{\hat{\epsilon}_{k,j} \mathcal{CN}(\hat{q}_{k,j}; 0, v_{q_{k,j}})}, \\ \psi(x) \triangleq \ln x - \frac{1}{2x} \end{cases}, \quad (13)$$

*Part 2 - MC part messages:* Firstly, we initialize the beliefs  $b(p_k^{10}) = \text{Be}(p_k^{10}; \hat{e}_k, \hat{f}_k)$  and  $b(p_k^{01}) = \text{Be}(p_k^{01}; \hat{c}_k, \hat{d}_k)$ , the parameters are updated later in (21). The MC downward messages are obtained by HMP rule [9, eqs. (5), (6)] as

$$m_{f_{S_{k,j}} \rightarrow s_{k,j}}^{\text{BP}}(s_{k,j}) = \xi_{k,j}^{\downarrow} \delta(1 - s_{k,j}) + (1 - \xi_{k,j}^{\downarrow}) \delta(s_{k,j}), \quad (14)$$

$$m_{s_{k,j} \rightarrow f_{S_{k,j+1}}}^{\text{BP}}(s_{k,j}) = \xi_{k,j}^{\downarrow} \delta(1 - s_{k,j}) + (1 - \xi_{k,j}^{\downarrow}) \delta(s_{k,j}), \quad (15)$$

where

$$\begin{cases} \xi_{k,1}^{\downarrow} \triangleq \frac{\exp\{\langle \ln p_k^{10} \rangle\}}{\exp\{\langle \ln p_k^{10} \rangle\} + \exp\{\langle \ln(1 - p_k^{10}) \rangle\}}, \\ \xi_{k,j}^{\downarrow} \triangleq \frac{\xi_{k,j-1}^{\downarrow} c_1 + (1 - \xi_{k,j-1}^{\downarrow}) c_2}{\xi_{k,j-1}^{\downarrow} (c_1 + c_4) + (1 - \xi_{k,j-1}^{\downarrow}) (c_2 + c_3)}, \\ \xi_{k,j}^{\downarrow} \triangleq \frac{\xi_{k,j}^{\downarrow} \bar{\pi}_{k,j}}{\xi_{k,j}^{\downarrow} \bar{\pi}_{k,j} + (1 - \xi_{k,j}^{\downarrow}) (1 - \bar{\pi}_{k,j})}, \end{cases}, \quad (16)$$

here,  $c_1, c_2, c_3, c_4$  denote the constants and defined as

$$\begin{cases} c_1 = \exp\{\langle \ln(1 - p_k^{01}) \rangle\}; & c_2 = \exp\{\langle \ln p_k^{10} \rangle\}; \\ c_3 = \exp\{\langle \ln(1 - p_k^{10}) \rangle\}; & c_4 = \exp\{\langle \ln p_k^{01} \rangle\}. \end{cases} \quad (17)$$

where  $\langle \ln x \rangle_{\text{Be}(x;a,b)} = \psi(a) - \psi(a+b)$ ,  $\langle \ln(1-x) \rangle_{\text{Be}(x;a,b)} = \psi(b) - \psi(a+b)$ .

Similarly, the MC upward messages passed between  $s_{k,j}$  and  $f_{s_{k,j}}$  can be computed by [9, eqs. (5), (6)], obtaining

$$n_{s_{k,j} \rightarrow f_{s_{k,j}}}^{\text{BP}}(s_{k,j}) = \xi_{k,j}^{\uparrow} \delta(1 - s_{k,j}) + (1 - \xi_{k,j}^{\uparrow}) \delta(s_{k,j}), \quad (18)$$

$$m_{f_{s_{k,j+1}} \rightarrow s_{k,j}}^{\text{BP}}(s_{k,j}) = \xi_{k,j}^{\uparrow} \delta(1 - s_{k,j}) + (1 - \xi_{k,j}^{\uparrow}) \delta(s_{k,j}), \quad (19)$$

where

$$\begin{cases} \xi_{k,j}^{\uparrow} \triangleq \bar{\pi}_{k,j}, & \xi_{k,j}^{\downarrow} \triangleq \frac{\xi_{k,j}^{\uparrow} \bar{\pi}_{k,j}}{\xi_{k,j}^{\uparrow} \bar{\pi}_{k,j} + (1 - \xi_{k,j}^{\uparrow})(1 - \bar{\pi}_{k,j})}, \\ \xi_{k,j}^{\downarrow} \triangleq \frac{\xi_{k,j+1}^{\uparrow} c_1 + (1 - \xi_{k,j+1}^{\uparrow}) c_4}{\xi_{k,j+1}^{\uparrow} (c_1 + c_2) + (1 - \xi_{k,j+1}^{\uparrow}) (c_3 + c_4)}, \end{cases} \quad (20)$$

here  $c_1, c_2, c_3, c_4$  are the same as (17).

*Part 3 - Transition probability update part:* Given the messages  $p(p_k^{10})$  and  $p(p_k^{01})$ , we can update the MC transition probability parameters using the method in [9, Part 4 within Section 4], the beliefs update by  $b(p_k^{10}) \propto \text{Be}(p_k^{10}; \hat{e}_k, \hat{f}_k)$  and  $b(p_k^{01}) \propto \text{Be}(p_k^{01}; \hat{c}_k, \hat{d}_k)$ , where the parameters are updated through

$$\begin{cases} \hat{e}_k = B_{s_{k,1}} + e_k + \sum_{j=2}^J \frac{B_{k,j}^{10}}{\rho_{k,j}}, & \hat{c}_k = c_k + \sum_{j=2}^J \frac{B_{k,j}^{01}}{\rho_{k,j}}, \\ \hat{f}_k = 1 - B_{s_{k,1}} + f_k + \sum_{j=2}^J \frac{B_{k,j}^{00}}{\rho_{k,j}}, & \hat{d}_k = d_k + \sum_{j=2}^J \frac{B_{k,j}^{11}}{\rho_{k,j}}. \end{cases} \quad (21)$$

and the parameters  $B_{s_{k,1}}, B_{k,j}^{00}, B_{k,j}^{01}, B_{k,j}^{10}, B_{k,j}^{11}, \rho_{k,j}$  can be calculated by [9, eq. (40)].

*Part 4 - Variance update part:* The message going out of the MC from  $s_{k,j}$  to  $f_{B_{k,j}}$  can be computed by [9, eq. (6)]

$$n_{s_{k,j} \rightarrow f_{B_{k,j}}}^{\text{BP}}(s_{k,j}) = \bar{\pi}_{k,j} \delta(1 - s_{k,j}) + (1 - \bar{\pi}_{k,j}) \delta(s_{k,j}), \quad (22)$$

where

$$\bar{\pi}_{k,j} \triangleq \frac{\xi_{k,j}^{\uparrow} \xi_{k,j}^{\downarrow}}{\xi_{k,j}^{\uparrow} \xi_{k,j}^{\downarrow} + (1 - \xi_{k,j}^{\uparrow})(1 - \xi_{k,j}^{\downarrow})}. \quad (23)$$

To update the variance of the BG-MC model, we have to calculate the combined belief  $b(b_{k,j}, s_{k,j})$  using [9, eq. (8)] as

$$b(b_{k,j}, s_{k,j}) = (1 - B_{b_{k,j}, s_{k,j}}) \delta(s_{k,j}) \delta(b_{k,j}) + B_{b_{k,j}, s_{k,j}} \delta(1 - s_{k,j}) \mathcal{CN}(b_{k,j}; \hat{\mu}_{k,j}, \vartheta_{k,j}), \quad (24)$$

where

$$\begin{cases} B_{b_{k,j}, s_{k,j}} \triangleq \frac{\bar{\pi}_{k,j} \text{temp}_{k,j}}{\bar{\pi}_{k,j} \text{temp}_{k,j} + (1 - \bar{\pi}_{k,j})}, \\ \vartheta_{k,j} = (v_{q_{k,j}}^{-1} + \frac{\hat{e}_{k,j}}{\hat{\eta}_{k,j}})^{-1}, & \hat{\mu}_{k,j} = \frac{\hat{q}_{k,j}}{v_{q_{k,j}}} \vartheta_{k,j}. \end{cases} \quad (25)$$

and the temporary variable  $\text{temp}_{k,j}$  is defined in (13).

Then, the message from  $f_{B_{k,j}}$  to variable node  $v_{k,j}$  can be computed with the HMP rule [9, eq. (7)] as

$$\begin{aligned} m_{f_{B_{k,j}} \rightarrow v_{k,j}}^{\text{MF}}(v_{k,j}) \\ \propto \text{Ga}(v_{k,j}; B_{b_{k,j}, s_{k,j}} + 1, B_{b_{k,j}, s_{k,j}} (|\hat{\mu}_{k,j}|^2 + \vartheta_{k,j})). \end{aligned} \quad (26)$$

Given  $m_{f_{v_{k,j}} \rightarrow v_{k,j}}^{\text{MF}}(v_{k,j}) = \text{Ga}(v_{k,j}; \epsilon_{k,j}, \eta_{k,j})$ , we can update the belief as  $b(v_{k,j}) = \text{Ga}(v_{k,j}; \hat{\epsilon}_{k,j}, \hat{\eta}_{k,j})$ , where parameters are updated through

$$\begin{cases} \hat{\epsilon}_{k,j} = \epsilon_{k,j} + B_{b_{k,j}, s_{k,j}}, \\ \hat{\eta}_{k,j} = \eta_{k,j} + B_{b_{k,j}, s_{k,j}} (|\hat{\mu}_{k,j}|^2 + \vartheta_{k,j}). \end{cases} \quad (27)$$

With the parameters updated in (27), we can compute the message from  $f_{B_{k,j}}$  to  $b_{k,j}$  by HMP rule [9, eq. (5)]. Finally, we can get the belief  $b(b_{k,j}) = (1 - B_{b_{k,j}}) \delta(b_{k,j}) + B_{b_{k,j}} \mathcal{CN}(b_{k,j}; \hat{\mu}_{k,j}, \vartheta_{k,j})$ . with the parameter  $B_{b_{k,j}} = B_{b_{k,j}, s_{k,j}}$ . Then, the algorithm outputs the mean and variance of the belief  $b(b_{k,j})$  as

$$\begin{cases} \hat{b}_{k,j} = \langle b_{k,j} \rangle_{b(b_{k,j})} = B_{b_{k,j}} \hat{\mu}_{k,j}, \\ v_{b_{k,j}} = B_{b_{k,j}} (|\hat{\mu}_{k,j}|^2 + \vartheta_{k,j}) - |\hat{b}_{k,j}|^2. \end{cases} \quad (28)$$

---

### Algorithm 1: GAMP-BG-MC algorithm

---

**Input:** Received signal  $\mathbf{Y}$ , channel matrix  $\mathbf{H}$ , iteration number  $T$ .  
**Output:** Decoding results  $\hat{b}_{k,j}, \forall k, j$ .  
**Initialize:** Prior parameters:  $\epsilon_{k,j}, \eta_{k,j}, \forall k, j; e_k, f_k, c_k, d_k, \forall k$ .  
 Belief parameters:  $\hat{\epsilon}_{k,j}, \hat{\eta}_{k,j}, \forall k, j; \hat{e}_k, \hat{f}_k, \hat{c}_k, \hat{d}_k, \xi_{k,j}^{\uparrow}, \forall k$ .  
 1 **while** convergence == FALSE OR iteration number <  $T$  **do**  
   // Part 1 - GAMP part messages  
 2 Run [15, Algorithm 1] and output  $v_{q_{k,j}}, \hat{q}_{k,j}, \forall k, j$   
 3  $\forall k, j$ : update  $\bar{\pi}_{k,j}$  by (13)  
   // Part 2 - MC part messages  
 4  $\forall k$ : update  $\xi_{k,1}^{\downarrow}$  by (16)  
 5  $\forall k, j \in [2 : J]$ : update  $\xi_{k,j}^{\downarrow}$  by (16)  
 6  $\forall k, j$ : update  $\xi_{k,j}^{\uparrow}$  by (16)  
 7  $\forall k, j \in [J - 1 : 1]$ : update  $\xi_{k,j}^{\uparrow}$  and  $\xi_{k,j}^{\downarrow}$  by (20)  
   // Part 3 - Transition probability update part  
 8  $\forall k, j$ : update  $B_{s_{k,1}}, B_{k,j}^{00}, B_{k,j}^{01}, B_{k,j}^{10}, B_{k,j}^{11}, \rho_{k,j}$  by (40) in [9]  
 9  $\forall k$ : update  $\hat{e}_k, \hat{f}_k$  and  $\hat{c}_k, \hat{d}_k$  by (21)  
 10 perform lines 4-7 again  
   // Part 4 - Variance update part  
 11  $\forall k, j$ : update  $\bar{\pi}_{k,j}$  by (23)  
 12  $\forall k, j$ : update  $B_{b_{k,j}, s_{k,j}}$  and  $\hat{\mu}_{k,j}, \vartheta_{k,j}$  by (25)  
 13  $\forall k, j$ : update  $\hat{\epsilon}_{k,j}, \hat{\eta}_{k,j}$  by (27)  
 14  $\forall k, j$ : update  $B_{b_{k,j}}$  and  $\hat{\mu}_{k,j}, \vartheta_{k,j}$  by (25) again based on new updated line 13  
 15  $\forall k, j$ : update  $\hat{b}_{k,j}, v_{b_{k,j}}$  by (28)

---

### B. Message Passing Scheduling

We summarize the proposed GAMP-BG-MC algorithm as shown in **Algorithm 1**. Specifically, the *Part 1* messages are first calculated in parallel at each time slot, which contains the [15, Algorithm 1] and the message going into the *Part 2*. Then we calculate the MC messages in sequence in lines 4-7. In *Part 3*, the parameters of  $p_k^{10}, p_k^{01}$  can be updated in lines 8-10. After that, we can improve the accuracy of the outgoing messages in *Part 4* by updating the MC part messages again based on the updated hyperparameters  $p_k^{10}, p_k^{01}$ . In the final step, we update the parameters of variances and calculate the output estimated data  $\hat{b}_{k,j}, \forall k, j$  with lines 12-15 in *Part 4*.

## IV. SIMULATION RESULTS

In this section, we compare the performance of the proposed GAMP-BG-MC algorithm. As a benchmark, we consider

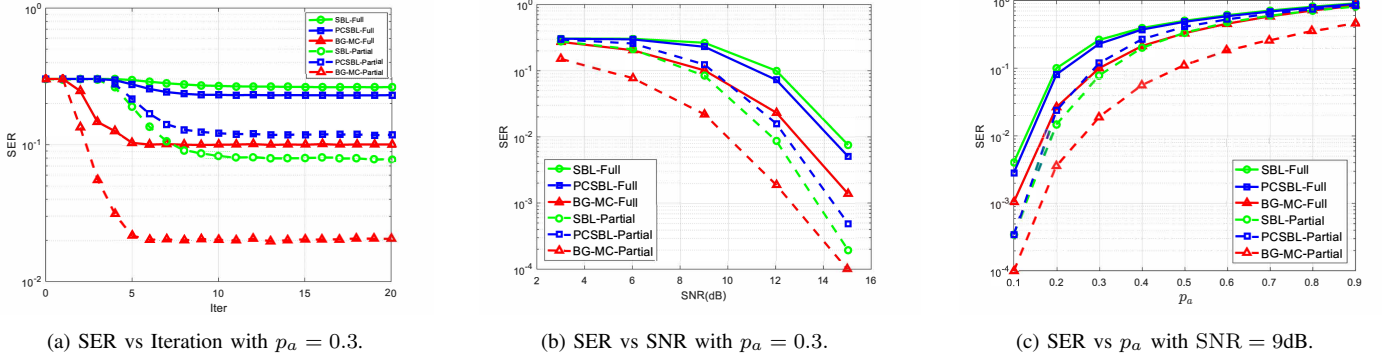


Fig. 3: Performance of proposed GAMP-BG-MC algorithm.

the state-of-the-art algorithms GAMP-SBL [7], [8], GAMP-PCSBL [8] referred as SBL and PCSBL in the following. Referring to [8], we consider the BPSK modulation scheme in all simulations, the UE number  $K = 20$ , the spreading factor  $N = 30$ , and the number of the continuous time slots  $J = 6$ . In experiments, we design two scenarios compared with the benchmark algorithms, one is the UE activity with temporal correlation, i.e., the UE will transmit the data partially during the whole frame, here denoted as "Partial". The other is an extreme phenomenon, the UE keeps transmitting data fully to the frame, referred to as "Full".

For the initialization, according to [9], the prior parameters are  $\{\epsilon_{k,j} = \eta_{k,j} = 1, \forall k, j\}$ ,  $\{e_k = f_k = c_k = d_k = 1, \forall k\}$ ,  $\xi_{k,j}^\uparrow = 1/2, \forall k, j$ , and the belief parameters are initialized with the same values of the priors. All the experiments are obtained by averaging  $\text{sim} = 1000$  Monte Carlo realizations. We use the symbol error rate (SER) defined as  $\text{SER} = \log_{10}(\frac{K_{err}}{\text{sim} \times K})$  as a performance metric,  $K_{err}$  is the number of UE whose symbol is erroneously decoded. The per-iteration complexity of the BG-MC is  $\mathcal{O}((N+1)KJ)$ , and it is in the same order as the SBL and PCSBL. But the iteration number of the BG-MC will always be small, as shown in Fig. 3 (a).

Fig. 3 (a) gives the convergence speed of the three algorithms under the SNR = 9dB. The proposed BG-MC algorithm has the fastest convergence speed compared with the SBL and PCSBL algorithms in both two scenarios. In Fig. 3 (b), we compare the average SER performance as a function of the SNRs. The simulation results show that the BG-MC algorithm performs better in the two scenarios. Further, we can find that the PCSBL is better than the SBL in the second scenario and the PCSBL is efficient in characterizing the block sparse structure, while the BG-MC is more accurate not only in the block sparse structure but also in the cluster sparse structure. The reason is that the BG-MC can update the statistic parameters automatically, which is suitable for the practice system. Fig. 3 (c) shows the SER performances as a function of the UE active rate  $p_a$  under SNR = 9dB. The BG-MC algorithm outperforms the benchmark algorithms in almost all ranges of  $p_a$ , especially in the first scenario.

## V. CONCLUSION

In this paper, we developed the BG-MC model to accurately characterize the slow change feature of the UE AS under the

GF-NOMA system. Based on the HMP rule, we designed the GAMP-BG-MC algorithm and tested it with the two scenarios. Experiments show that the proposed algorithm achieves better SER performance. Hence, the proposed technique can be deployed for the URLLC in the 6G and beyond.

## REFERENCES

- [1] X. Chen, *et al.*, "Massive access for 5G and beyond," *IEEE J. Sel. Areas Commun.*, vol. 39, no. 3, pp. 615–637, Mar. 2021.
- [2] L. Dai, *et al.*, "Non-orthogonal multiple access for 5G: solutions, challenges, opportunities, and future research trends," *IEEE Commun. Mag.*, vol. 53, no. 9, pp. 74–81, Sep. 2015.
- [3] L. Liu, *et al.*, "Sparse signal processing for grant-free massive connectivity: A future paradigm for random access protocols in the internet of things," *IEEE Signal Process. Mag.*, vol. 35, no. 5, pp. 88–99, Sep. 2018.
- [4] B. Li, *et al.*, "Compressed sensing based multiuser detection of grant-free NOMA with dynamic user activity," *IEEE Commun. Lett.*, vol. 26, no. 1, pp. 143–147, Nov. 2021.
- [5] Y. Gao, *et al.*, "Multiuser detection of GF-NOMA with dynamic-active users and temporal-correlated channels," *IEEE Commun. Lett.*, vol. 26, no. 10, pp. 2380–2384, Jul. 2022.
- [6] W. Yuan, *et al.*, "Iterative joint channel estimation, user activity tracking, and data detection for FTN-NOMA systems supporting random access," *IEEE Trans. Commun.*, vol. 68, no. 5, pp. 2963–2977, Feb. 2020.
- [7] X. Zhang, *et al.*, "Bayesian learning-based multiuser detection for grant-free NOMA systems," *IEEE Wireless Commun. Lett.*, vol. 21, no. 8, pp. 6317–6328, Feb. 2022.
- [8] X. Zhang, *et al.*, "Generalized approximate message passing based Bayesian learning detectors for uplink grant-free NOMA," *IEEE Trans. Veh. Technol.*, pp. 1–6, May 2023.
- [9] Y. Song, *et al.*, "Hybrid message passing algorithm for downlink FDD massive MIMO-OFDM channel estimation," *IEEE Trans. Wireless Commun.*, pp. 1–1, Oct. 2023.
- [10] X. Kuai, *et al.*, "Structured turbo compressed sensing for downlink massive MIMO-OFDM channel estimation," *IEEE Trans. Wireless Commun.*, vol. 18, no. 8, pp. 3813–3826, Aug. 2019.
- [11] C. I. Frison, *et al.*, "MC-CDMA and SCMA performance and complexity comparison in overloaded scenarios," *2019 IEEE Colombian Conference on Communications and Computing (COLCOM)*, pp. 1–6, Jun. 2019.
- [12] H. R. Carvajal Mora, *et al.*, "Mean bit error rate evaluation of MC-CDMA cellular systems employing multiuser-maximum-likelihood detector," *IEEE Trans. Veh. Technol.*, vol. 66, no. 11, pp. 9838–9851, Jul. 2017.
- [13] W. Zhu, *et al.*, "Message passing-based joint user activity detection and channel estimation for temporally-correlated massive access," *IEEE Trans. Commun.*, vol. 71, no. 6, pp. 3576–3591, Mar. 2023.
- [14] N. L. Pedersen, *et al.*, "Application of Bayesian hierarchical prior modeling to sparse channel estimation," in *Proc. IEEE Int. Conf. Commun. (ICC)*, Jun. 2012, pp. 3487–3492.
- [15] L. Mo, *et al.*, "Generalized unitary approximate message passing for double linear transformation model," *IEEE Trans. Signal Process.*, vol. 71, pp. 1524–1538, Apr. 2023.